Heliyon 10 (2024) e32181

Contents lists available at ScienceDirect

Heliyon

journal homepage: www.cell.com/heliyon

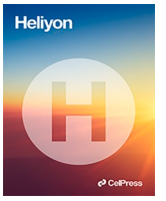

Research article

Evaluation of the SERS performances of Tabun and VX label-free detection in complex and multicomponent fluids

Giulia Zappalà [a,*], Elodie Dumont [a,d], Gohar Soufi [a,d], Nora Molander [b], Amirali Abbaspourmani [c], Damir Asoli [c], Per Ola Andersson [b], Tomas Rindzevicius [a,c], Anja Boisen [a,d]

[a] The Danish National Research Foundation and Villum Foundation's Center for Intelligent Drug Delivery and Sensing Using Microcontainers and Nanomechanics (IDUN), Department of Health Technology, Technical University of Denmark, Denmark
[b] CBRN Defence and Security, Swedish Defence Research Agency, FOI, SE-90182, Umeå, Sweden
[c] Silmeco ApS, 2450, Copenhagen, Denmark
[d] BioInnovation Institute Foundation, Copenhagen N, 2200, Denmark

ARTICLE INFO

Keywords:
Surface-enhanced Raman scattering
Nerve agents
Fast response
Performance assessment
Portable devices
Real-life fluids

ABSTRACT

Nerve agents represent a serious threat to security worldwide. Chemical terrorism has become an alarming danger since the technological progresses have simplified the production of nerve agents. Therefore, there is an immediate demand for a fast and precise detection of these compounds on-site and real-time. In this perspective, Surface-Enhanced Raman Scattering (SERS) has emerged as a well-suited alternative for on-field detection.

SERS performances of unfunctionalized SERS substrates were evaluated in realistic samples. Two nerve agents, Tabun and VX, were diluted in two matrix models: a contact lens solution, and a caffeine-based eye serum. The performance two research-grade instruments and two portable devices were compared. Despite the use of a small sampling volume of complex matrices without any sample pre-treatment, we achieved Tabun detection in both media, with a practical limit of detection (LOD) in the range of 7–9 ppm in contact lens liquid, and of 10.2 ppm in eye serum. VX detection turned out to be more challenging and was achieved only in contact lens solution, with a practical LOD in the range of 0.6–5 ppm.

These results demonstrate the feasibility of on-field detection of nerve agents with SERS, that could be implemented when there is suspicion of chemical threat.

1. Introduction

Chemical warfare agents (CWAs) are highly toxic compounds originally designed for military use [1]. Among CWAs, nerve agents are the most toxic synthetic compounds known. Nerve agents are organophosphorus compounds (OP) that were developed in the mid-to late-twentieth century [2]. The extreme toxicity of these compounds is associated to their capability to inhibit acetylcholinesterase (AChE), a cholinergic enzyme principally found at postsynaptic neuromuscular junctions [3]. The role of AChE is to hydrolyse acetylcholine (ACh), a neurotransmitter that stimulates the secretion of body fluids and the contraction of skeletal muscles. AChE terminates neuronal transmission and signalling between synapses, in order to prevent the continuous overstimulation of the receptors

* Corresponding author.
E-mail address: giuzap@dtu.dk (G. Zappalà).

https://doi.org/10.1016/j.heliyon.2024.e32181
Received 2 April 2024; Received in revised form 21 May 2024; Accepted 29 May 2024
Available online 31 May 2024

[4]. When AChE action is inhibited, muscles contract involuntarily, fluid secretions increase, and seizures can happen due to ACh accumulation in the peripheral and in the central nervous system [2,5,6].

Nerve agents are divided in two classes: i) G-agents where "G" stands for German [7], in which Tabun (GA), Sarin (GB), Soman (GD) and Cyclosarin (GF) are included; ii) V-agents where "V" stands for venomous [8], such as VX, VG and VR [1,9]. G-agents are moderately volatile and can represent a danger both as vapor and as liquid. V-agents are less volatile but persistent and, thus, constitute a liquid hazard [1,2]. When nerve agents are in vapor or aerosol form, the main routes of exposure are inhalation and dermal contact. In a liquid form, they can be absorbed through dermal contact, ocular absorption and ingestion [5,10]. Among the nerve agents, GA was the first of the G-agents that was synthesized in 1936 [11]. The main routes of exposure for GA are inhalation, dermal contact, and ocular absorption. In gas form, the median lethal concentration (LCt50) in humans has been assessed to be 135 $mg\ min\ m^{-3}$ at a respiratory minute volume (RMV) of 15 $l\ min^{-1}$ for 0.5–2 min and 200 $mg\ min\ m^{-3}$ at a resting RMV of 10 $l\ min^{-1}$. In liquid form, the percutaneous human median lethal dose (LD50) is predicted to be 21 $mg\ kg^{-1}$ (ppm) body mass [11]. On the other hand, the V-agent VX can be mainly absorbed through dermal and ocular contact, and, in this case, the human LD50 is assessed to be 0.315 $mg\ kg^{-1}$ (ppm) [12].

Nowadays, chemical terrorism has become a serious threat to security worldwide. After the use of GA in 1984 in the Iran-Iraq war [13], the Iraqi attack on the Kurdish civilians of Halabja [14], and the release of VX and Sarin in Japan on civilians in 11 occasions during 1994 and 1995 [15], the threat of nerve agents use in domestic terrorist attacks has become evident. Considering the technological progresses, the easy access to information online and the relative simplicity of nerve agent production, there is an urgent need for a fast and precise detection of these types of OP compounds.

Over the past few decades, numerous techniques have been employed for the detection of OP compounds such as gas chromatography (GC) [16], liquid chromatography (LC) [17], Fourier transform infrared spectrometry (FTIR) [18], and ion mobility spectrometry (IMS) [19]. Although these methods showed an adequate sensitivity and robustness, they are not suited for on-field detection due to the necessary bulky and cumbersome instruments, the required trained personnel to operate them, and the elaborate and time-consuming sample preparation [20]. In recent years, fluorescent probes [21], surface acoustic wave sensors [22], and electrochemical biosensors [23] have been employed for on-site detection of nerve agent. However, they usually lack sensitivity or selectivity [24]. One of the most promising techniques to detect OP has become Surface-Enhanced Raman Scattering (SERS), a label-free, sensitive, and selective method that exhibits several advantages in terms of speed, cost, and portability. SERS provides fast response and a chemical fingerprint information of target molecules absorbed on nanostructured noble metal surfaces. The sensing of the absorbed analytes can reach low limits of detection, or even single molecule detection [25]. In the SERS technique, the Raman signal is mainly enhanced through electromagnetic enhancement (EM), which results from a high electric field due to localized surface plasmon resonance (LSPR) of the metal nanostructures [26]. SERS has been used in numerous applications in different fields, such as food chemistry [27], therapeutic drug monitoring [28], environmental monitoring [29], and medicine [30]. SERS has also shown a great potential for on-site detection of CWAs, thanks to the availability of miniaturized, handheld Raman systems. Various studies have employed SERS in nerve agent detection, especially for VX that can represent a threat regarding contamination of water supplies [31,32]. In those studies, VX has been tested either in a simple matrix such as pure water [32], or more complex matrix pre-treated in advance, such as lake water previously filtrated with Nylon filters of few μm pore size [31]. Many other studies have been focusing on surface modification of the SERS substrates to overcome the weak interaction of OP compounds with the metals [26,33]. Surface modification can, indeed, increase selective adsorption of the analyte on the surface and enhance the sensitivity, but it also exhibits some drawbacks. Since the technique sometimes involves multiple steps, the process can become time-consuming, and, at the same time, it can introduce variability, inhomogeneity, and many constraints in terms of reaction and storage conditions and applicable molecules [34]. However, not only the weak interaction, but also the matrix in which OP compounds are dispersed must be taken into account. The presence of various ions, proteins, and polysaccharides in the matrix can affect SERS performance, causing an increment in the limit of detection (LOD) and producing artefacts in SERS spectra. The competitive adsorption between analytes and interfering chemical species or the formation of complexes between sample molecules and ions can decrease molecule adsorption on the surface and be the cause of the matrix effect [35].

To assess the effectiveness of SERS for on-site detection in real-life scenario, it is fundamental to evaluate SERS performances of unfunctionalized SERS substrates in more realistic matrixes. Unlike labelled detection, label-free SERS indeed benefits from fingerprint characteristics of the SERS spectra and can therefore be of great help in identifying an unknown threat.

Therefore, in this paper, we tested Si-based Au Nanopillar (NP) SERS substrates for the detection of GA and VX in two different matrix models: a contact lens solution (renu® multi-purpose solution [36]), and a caffeine-based eye serum (Apolosophy Active + Caffeine Eye Serum [37]). The two solutions were chosen to mimic a near real-life scenario of a possible terroristic attack to civilians, where OP would be dispersed in everyday life fluids such as cosmetics. Moreover, the composition of those fluids is complex and can thus interfere with SERS spectra, leading to a more complicated detection. The evaluation of SERS performance in multicomponent fluids was performed both with two research-grade Raman spectrometers (LabRAM 800 H/R and DXRxi Raman Imaging Microscope) and with two portable systems (MiniRAMAN microscope and FirstDefender™ RMX). The main objective of this work was, thus, to establish the benefit of SERS for the detection of nerve agents in a near real-life case scenario and to compare the performance of research-grade Raman spectrometers with portable instruments that can be used for on-site detection. We demonstrated that GA was detectable in both matrices with practical LOD values lower than the GA LD50 in humans even with the portable devices. The detection of VX proved to be more challenging than the one of GA, most probably due to: (i) a lower affinity of VX to the Au surface or (ii) a higher susceptibility to interfering compounds present in the matrix. VX detection was achieved in the contact lens liquid, while it was not feasible in eye serum due to a more intense matrix effect derived from this medium.

2. Materials and methods

2.1. SERS substrates: fabrication and characterization

The SERS substrates employed in this study were Si-based Au NPs. The Au NP SERS substrates were fabricated using a two-step fabrication process: maskless reactive ion etching (RIE) of Si and electron (e)-beam evaporation of Au, as described in Refs. [38, 39]. Briefly, a single side polished 6-inch Si wafer was etched in a SF_6 and O_2 gas mixture flow during a maskless RIE process in an ICP Metal Etch system (PRO ICP, SPTS Technologies Ltd., Newport, UK). In this study, two Si NP structure designs were fabricated. The first design presented the following features: NP density ~26 NP/μm^2, NP height ~400 nm, NP width ~50 nm. The second one had a NP density of ~14 NP/μm^2, a NP height of ~750 nm and a NP width of ~60 nm. The NPs were then coated with 160 nm of Au, using a Temescal FC-2000 e-beam evaporator from Ferrotec (Livermore, CA, USA). The fabrication process resulted in Au-capped Si NP SERS substrates. The processed 6-inch Si wafers were then diced from the backside into 3 × 3 mm^2 chips using a laser micromachining tool (D-09126, 3D-Micromac AG, Chemnitz, Germany). The Au NP SERS substrates were stored under nitrogen.

2.2. Nerve agents and multicomponent fluids

GA and VX (98.1 % purity analysed with gas chromatography/mass spectrometry (GC/MS) as in Ref. [31], synthesized by the Swedish Defence Research Agency) were solubilized in acetonitrile (ACN) 10 % v/v to prepare a stock solution of 1000 ppm. ACN was of analytical grade and purchased from Sigma-Aldrich (Merck KGaA, Darmstadt, GER). First, GA was diluted in Milli-Q water from Milli-Q Advantage A10 purification system (Merck KGaA, Darmstadt, GER) to a concentration of 100 ppm, 10 ppm and 5 ppm directly before the measurements.

To prepare the other standards, two different commercially available solutions were used: renu® multi-purpose solution [36], and Apolosophy Active + Caffeine Eye Serum [37].

The contact lens solution is a sterile, isotonic solution that contains hydroxyalkylphosphonate (HYDRANATE®), boric acid, edetate disodium, poloxamine, sodium borate and sodium chloride, and is preserved with 0.0001 % polyaminopropyl biguanide (DYMED®) [36]. GA stock solution was diluted in renu® solution to prepare standards of 200 ppm, 100 ppm, 50 ppm, 20 ppm, 10 ppm, and 5 ppm. VX stock solution was diluted in renu® solution to prepare standards of 100 ppm, 50 ppm, 35 ppm, 20 ppm, 10 ppm, and 5 ppm.

The caffeine-based eye serum contains water, caffeine, propanediol, maltodextrin, glycerin, lactic acid, hydroxyethyl cellulose, magnesium sulfate, chondrus crispus powder, xanthan gum, ethylhexylglycerin, and phenoxyethanol [37]. GA stock solution was diluted in the caffeine-based eye serum solution to prepare standards of 200 ppm, 100 ppm, 50 ppm, 20 ppm, and 10 ppm. VX stock solution was diluted in the caffeine-based eye serum solution to prepare standards of 200 ppm, 100 ppm, and 50 ppm.

2.3. Experimental procedure

Two different designs of Au NPs were used: (i) the wafers with the first design were freshly fabricated while (ii) the ones with the second design were fabricated 6 months before use. GA was tested on (i), while VX on (ii) due to limited amount of SERS substrates from each batch.

The SERS substrates were exposed to the two analytes through the droplet casting method. For both GA and VX, 3 μl of the analyte in the renu® solution and in the caffeine-based eye serum solution were pipetted onto 3 SERS substrates, and the droplet was left to evaporate on the surface before analysis. As control samples, 3 μl of a solution of ACN in the renu® solution and in the caffeine-based eye serum were drop casted each on 3 substrates.

Table 1
Raman equipment and parameters employed to analyse the SERS substrates.

	DXRxi Raman Imaging Microscope	LabRAM 800 H/R	MiniRAMAN microscope	FirstDefender™ RMX
Brand	Thermo Fisher Scientific (Waltham, MA, USA)	Horiba Scientific (Kyoto, Japan)	Lightnovo (Birkerød, Denmark)	Thermo Fisher Scientific (Waltham, MA, USA)
Type of device	Benchtop	Benchtop	Portable	Handheld
Laser wavelength	780 nm	785 nm	785 nm	785 nm
Objective	10X	10X	10X	Probe (Working distance 6 mm)
Nominal laser spot diameter	10 μm	5 μm	15 μm	100 μm
Power	24 mW	4 mW	4.5 mW	75 mW
Exposure time	50 ms	2 s	250 ms	1 s
Accumulations	1	10	2	1
Type of acquisition	Maps	Point measurements	Maps	Point measurements
Map size	3 × 3 mm^2	–	2.5 × 2.5 mm^2	–
Number of points per substrate	2500	3	625	1

2.4. Raman equipment and data analysis

Four Raman spectrometers were used to evaluate the SERS performance of the substrates: two research-grade benchtop and two portable instruments. The characteristics of each equipment and the parameters used are listed in Table 1.

The SERS data analysis was performed using a data analysis software developed using a combination of Delphi RAD Studio (Embarcadero Technologies, Austin, TX, USA) and Python (Python Software Foundation). Each spectrum was cropped between 600 cm^{-1} and 2300 cm^{-1} and background corrected with an asymmetric least square model between 600 cm^{-1} and 2300 cm^{-1} and a linear model in the spectral range between 2000 cm^{-1} and 2200 cm^{-1} for GA, and 750 cm^{-1} and 1000 cm^{-1} for VX. The mean value of the 2133 cm^{-1} (CN stretch vibration [40]) peak height for GA, and 915 cm^{-1} (CCN stretch or NC_3 stretch [32]) peak height for VX were calculated. For the data acquired with MiniRAMAN microscope and DXRxi Raman Imaging Microscope, an average of the peak intensity value was extracted from 3 maps, in which an intensity threshold was applied in order to consider only the droplet region on the SERS substrate surface. For LabRAM 800 H/R data, an average of the peak intensity value was extracted from 9 points (3 points per chip), while for FirstDefender™ RMX an average of 3 points (1 point per chip) was calculated. The data were plotted and fitted using logistic and linear function with Origin (2023, OriginLab Corporation, MA, USA).

The theoretical LODs for the different instruments were calculated as $3\sigma/s$, in which σ is the standard deviation (SD) of the intercept of the linear range, and s is the slope of the calibration curve. The limits of quantification (LOQs) were calculated as $10\sigma/s$. The practical LODs of the four instruments were calculated as the concentration attributed to three times the intensity of the blank signal.

3. Results and discussion

3.1. SERS analysis of GA in Milli-Q water and in multicomponent fluids

As shown in Fig. 1a, a preliminary investigation was conducted in Milli-Q water to determine the matrix effect on GA detection. To perform the analysis, six Au NP substrates were used: 3 μl of 10 ppm GA solutions in Milli-Q water, in contact lens liquid and in eye serum were casted on three substrates respectively, while 3 μl of ACN in Milli-Q water, in contact lens liquid and in eye serum were casted on other three substrates as control samples. The SERS maps were collected with the DXRxi Raman Imaging Microscope as previously described. The SERS spectra of GA in Milli-Q water, in renu® solution and in caffeine-based eye serum showed the characteristic peak at 2133 cm^{-1}, which was assigned to the CN stretch vibration [40], displayed in Fig. 1b. Comparing the spectra from Milli-Q water (shown on the first y-axis) and in the two sample matrices (shown on the second y-axis), it is evident how the complexity of the matrices leads to a consistent decrease of the whole SERS intensity signal and especially of the GA peak at 2133 cm^{-1} [40]. The eye serum matrix, in particular, decreases the SERS sensitivity with almost two orders of magnitude, if compared to water, and one order of magnitude, if compared to renu® solution, leading to a reduced SERS signal intensity of the characteristic GA spectral feature.

As it can be observed in Fig. 1a, a peak in the same location as GA appears also in the control sample (dashed lines). This can be expected from the presence of ACN, which, in Raman spectroscopy studies, have the same CN stretch vibration at a Raman shift of 2254 cm^{-1} [41]. When ACN was employed on Au SERS substrates, a new band appeared at 2137 cm^{-1}, which was assigned to surface

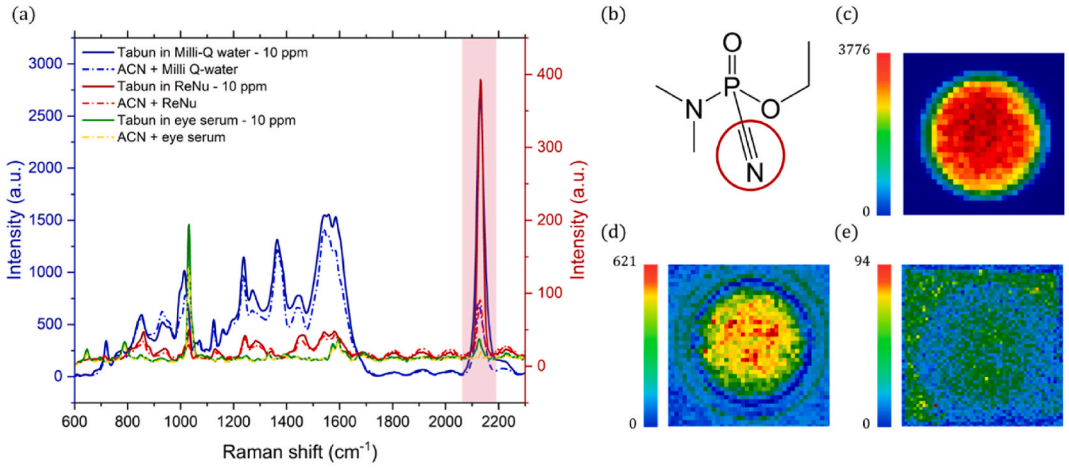

Fig. 1. (a) Averaged SERS spectra after drop casting 3 μl of 10 ppm GA solution in water (blue solid line), 3 μl of GA solution in contact lens solution (red solid line) 3 μl of GA solution in eye serum (yellow solid line), 3 μl of ACN in water (blue dashed line), 3 μl of ACN in contact lens solution (red dashed line), and 3 μl of ACN in eye serum (yellow dashed line) on Au NP substrates. All spectra were acquired with DXRxi Raman Imaging Microscope with 780 nm laser excitation wavelength, laser power of 24 mW, exposure time of 0.050 s, 1 accumulation, 3000 × 3000 μm^2 map and 60 μm step size. Spectra from the contact lens solution and eye serum are shown on the second (red) y-axis. (b) GA chemical structure. The 2133 cm^{-1} peak in the SERS spectrum was assigned to the CN stretch. (c) Representative 2133 cm^{-1} peak intensity distribution of a drop of GA in water on the SERS substrate. (d) Representative 2133 cm^{-1} peak intensity distribution of a drop of GA in renu® solution on the SERS substrate (e) Representative 2133 cm^{-1} peak intensity distribution of a drop of GA in eye serum on the SERS substrate.

cyanide species developed after ACN decomposition reactions on the surface [42]. Other Raman bands of GA are generally found around 710 cm^{-1} and 730 cm^{-1}, which are stemming from the phosphorus atom, and around 1269 cm^{-1} originating from the PO moiety [40]. However, in this study, those bands were not recorded, possibly due to the weak affinity of the agent to the surface. The multiple peaks present in the recorded spectra are most likely originating from the ACN contribution, surface contaminations and the substrate itself due to the maskless Si RIE process.

Fig. 1c–e illustrates the different intensity distributions on the SERS substrate of the GA peak at 2133 cm^{-1} when it was prepared in water, in renu® solution, and in eye serum, respectively. A different wetting of the surface occurs when the analyte is diluted in the contact lens liquid and, more notably, in the eye serum solution, probably because of the presence of surfactants in the matrix, which make the droplet spread on the substrate.

To further assess the effect of the renu® matrix on Au NPs, SEM characterization of the substrates was conducted. Fig. 2 shows the difference between pristine substrate (Fig. 2a), and substrates covered by 3 μl of renu® solution (Fig. 2 b-d). The contact lens solution is a thick matrix that, when it dries on the NPs, leaves only small cluster of NPs uncovered, which leads to a reduced plasmonic response. In Fig. 2c and d, the cross section of a substrate can be observed. An approximately 14 μm thick layer, probably caused by polymers and salts present in the lens solution, covers many NPs. This can reduce the probability of the analyte getting in close contact with the metal cap and prevent the leaning of the NPs and consequently the hot-spot formation.

The challenging GA detection both in renu® solution and in caffeine-based eye serum represents ideal cases for mimicking near real-life scenarios.

3.2. SERS performance evaluation of GA detection in complex matrices

After having determined the magnitude of the matrix effect and the position of the analyte's characteristic peaks on the Au NPs, the performance of the SERS substrates for GA detection in un-treated matrices was evaluated. Sample pre-treatment was not considered in this work, in order to provide a fast on-site detection method.

GA was measured in the two conditions previously described: diluted in renu® contact lens solution and in caffeine-based eye serum. Fig. 3a shows the averaged SERS spectra of a map recorded with DXRxi Raman Imaging Microscope after drop casting 3 μl of 200 ppm, 100 ppm, 50 ppm, 20 ppm, 10 ppm, and 5 ppm GA solution in contact lens solution. The SERS spectra of GA in contact lens liquid recorded with the other instruments can be found in Figs. S1, S2 and S3. As it can be better observed in Fig. 3b, GA characteristic peak intensity is not linearly increasing with the concentration, probably saturated by the limited available area covered with NP and left intact from renu® solution matrix. Fig. 3c shows the averaged SERS of GA dilutions in eye serum and how it leads to a decreased SERS sensitivity of the characteristic GA spectral feature (Fig. 3d). The same behaviour can be observed in the spectra recorded with the other pieces of equipment in Figs. S4 and S5. Competitive adsorption between GA and the substances contained in Apolosophy Active + Caffeine Eye Serum might be one of the causes of the weak signal. As evident in Fig. 3c–a major peak appears in the spectrum at 1032 cm^{-1}, which can be assigned to the in-plane C–C deformation [43] of caffeine [37]. Caffeine has indeed been reported as having a high affinity for Au and Ag SERS substrates [43] and is therefore expected to highly compete with GA for adsorption on the SERS substrate. In addition, the eye serum was much more viscous than the lens solution, due to the presence of many polymers in its

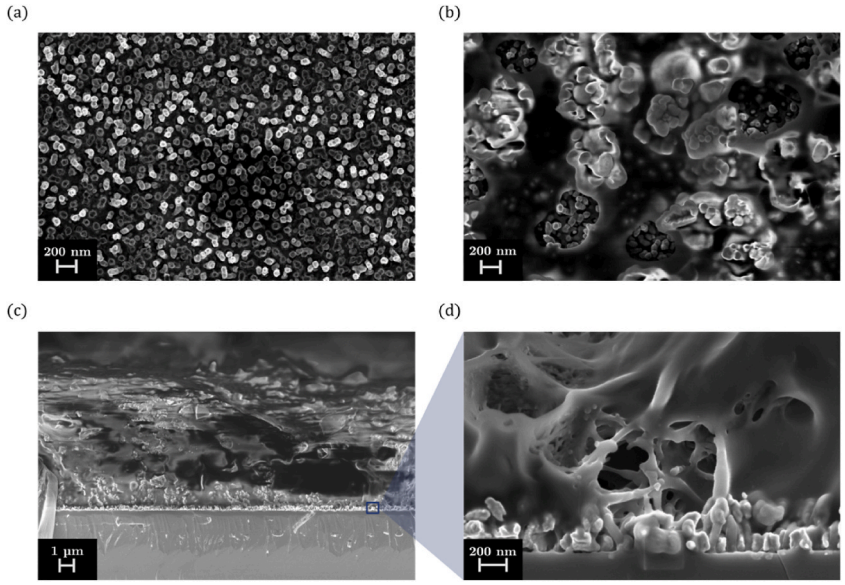

Fig. 2. SEM images of Au NPs. (a) Top-down view of pristine Au NPs (50K magnification). (b) Top-down view of Au NPs with 3 μl renu® solution dried on top (50K magnification). (c) Cross section of Au NPs covered with renu® solution (10K magnification). (d) Cross section detail (100K magnification) of Au NPs covered with renu® solution.

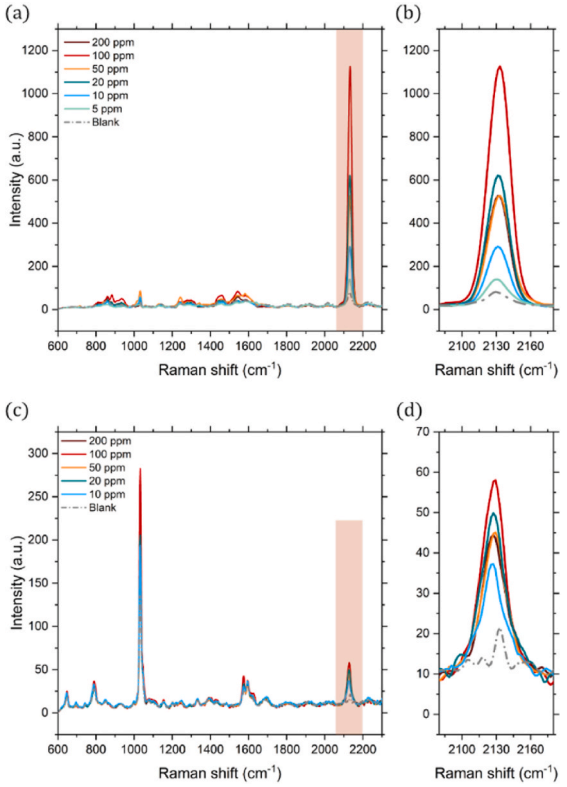

Fig. 3. (a) Averaged SERS spectra after drop casting 3 μl of 200 ppm, 100 ppm, 50 ppm, 20 ppm, 10 ppm and 5 ppm GA solution in contact lens solution (solid lines) and 3 μl of ACN in contact lens solution (grey dashed line) on Au NP substrates. (b) Concentration-dependent intensity of the peak at 2133 cm^{-1} for GA in the contact lens solution. (c) Averaged SERS spectra after drop casting 3 μl of 200 ppm, 100 ppm, 50 ppm, 20 ppm, and 10 ppm GA solution in eye serum solution (solid lines) and 3 μl of ACN in eye serum solution (grey dashed line) on Au NP substrates. (d) Concentration-dependent intensity of the peak at 2133 cm^{-1} for GA in eye serum solution. All spectra were acquired with DXRxi Raman Imaging Microscope (parameters in Table 1).

formulation, which could in turn form a thicker deposit on the SERS substrate and hinder SERS detection.

The two matrices influence the vibrational bands in the fingerprint region, lowering the SERS signal intensity, and introducing additional bands from their constituents, leading to a more complex detection of the analyte. However, despite this matrix effect, it was still possible to detect GA in those two solutions without adding any sample pre-treatment. The main SERS active GA band is fortunately located in the silent region, i.e. between 1800 and 2800 cm^{-1}, where only specific chemical functions, such as cyano or alkynyl, display a clear and intense Raman response [44]. In this way, GA characteristic peak remains cleared from interfering SERS signals.

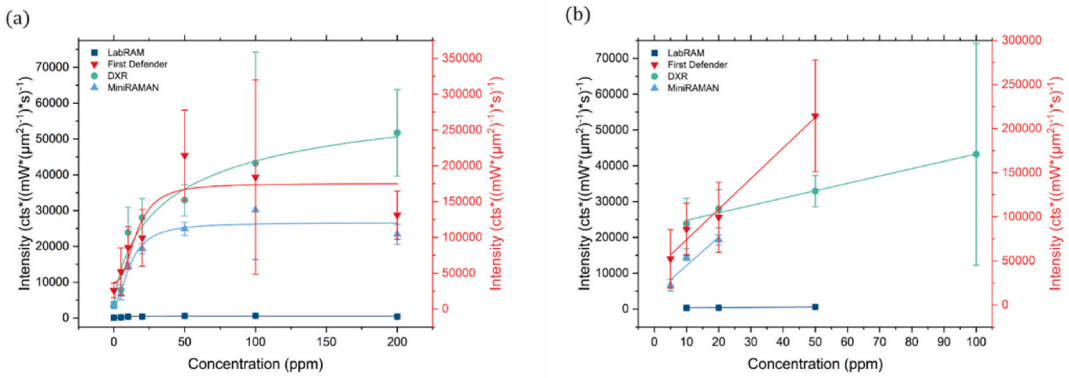

Fig. 4. (a) GA 2133 cm^{-1} peak intensity vs. concentration curves in contact lens solution performed using different Raman equipments. A logistic function was used to fit SERS data. (b) Detection range of the calibration curves. The data acquired with FirstDefender™ RMX are shown in red on the second y-axis.

Therefore, evaluation of the detection performances was performed in un-treated matrices in the following step.

3.2.1. *Performance assessment in renu® multi-purpose solution*

Detection of GA in renu® contact lens solution was carried out on Au NPs from the first design, and three chips were analysed for every concentration. The SERS signal from drop casted solutions on the surfaces was recorded with the four Raman spectrometers listed in Table 1. Fig. 4a shows GA 2133 cm^{-1} characteristic signal intensity vs. concentration curves in contact lens solution after normalizing the SERS signal intensity, recorded from the different Raman instruments, by power density and exposure time. The SERS signal intensity started to saturate after 50 ppm for the research-grade device LabRAM 800 H/R and for the portable FirstDefender™ RMX and MiniRAMAN microscope. For the DXRxi Raman Imaging Microscope, the intensity saturated at 100 ppm, concentration for which an extremely high SD between triplicates highlighted unrepeatability of the measurements.

In Fig. 4b, the detection range of the calibration curve for every equipment is enlarged. A linear correlation between concentration and intensity was obtained between 5 ppm and 50 ppm for FirstDefender™ RMX with an R^2 of 0.983. The DXRxi Raman Imaging Microscope showed a detection range from 10 ppm to 100 ppm, with an R^2 of 0.990. In Table S1, the linear equation, the R^2, p-value, theoretical LOD, practical LOD, theoretical LOQ, analytical sensitivity, detection range, and average relative standard deviation (RSD) values are shown for DXRxi Raman Imaging Microscope and FirstDefender™ RMX. The theoretical LOD and LOQ were 7.60 ppm and 25.34 ppm for the portable device, while they were 12.31 ppm and 41.04 ppm for the research-grade one. In order to assess sensitivity and precision of the spectrometers, the analytical sensitivity was calculated. FirstDefender™ RMX showed an analytical sensitivity 4 times higher than DXRxi Raman Imaging Microscope, giving the best performance in GA detection in contact lens solution. Those results could be explained by the larger substrate surface analysed by the FirstDefender™ RMX, which provided a more accurate average of the GA response on the SERS substrates. However, FirstDefender™ RMX exhibited the highest RSD value, which gives an indication on the decreased repeatability of quantitative measurements on a portable instrument compared to a research-grade device. This might be due to human error derived from the handling of the device during the measurements in order to keep it at the same working distance for every measurement.

In the other two cases, when using LabRAM 800 H/R and MiniRAMAN microscope, during the investigation of the p-value, it was found that the null hypothesis could not be rejected and, considering a confidence level of 95 %, there was no linear correlation

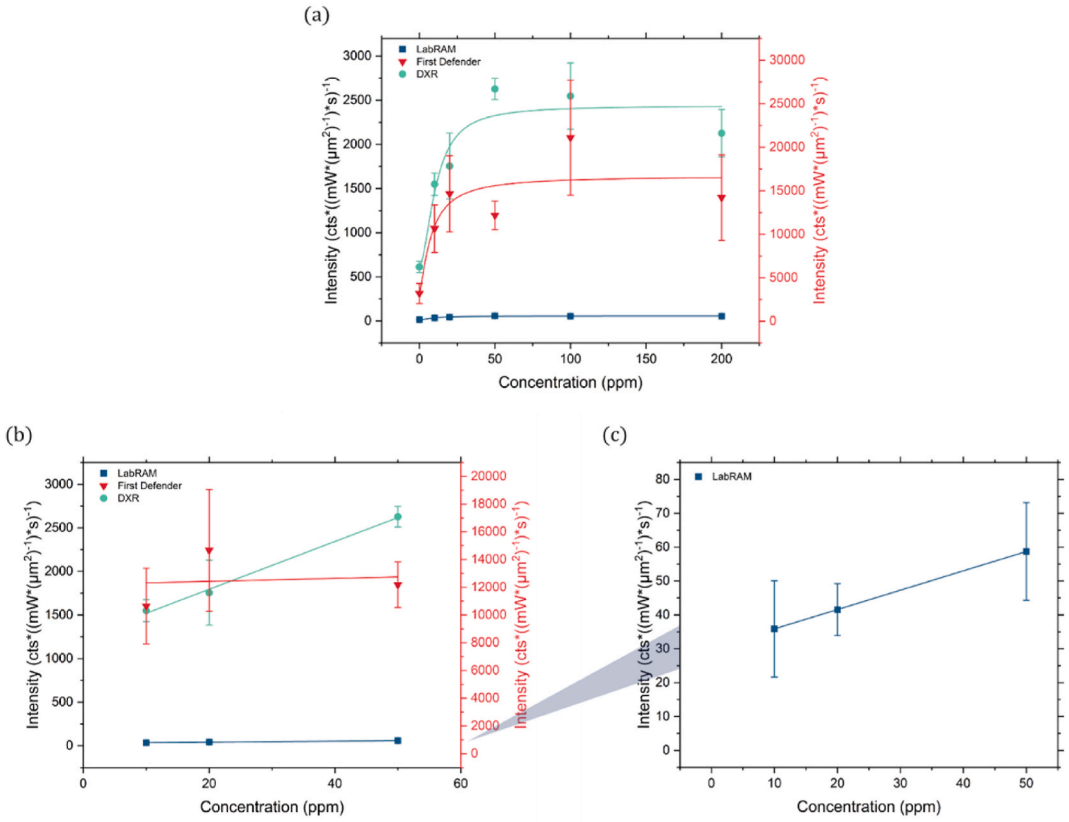

Fig. 5. (a) GA 2133 cm^{-1} peak intensity vs. concentration curves in eye serum solution performed using different Raman pieces of equipment. A logistic function was used to fit SERS data. (b) Detection range of the calibration curves. The data acquired with FirstDefender™ RMX are shown in red on the second y-axis. (c) Enlargement of the calibration curve acquired with LabRAM 800 H/R.

between signal and concentrations. Since the purpose of the study was detection of the compound in un-treated matrices and unfunctionalized substrates, a practical LOD was calculated for all pieces of equipment. The practical LOD represents the concentration that gives as a response three times the signal intensity of the blank sample. When considering this LOD, the four instruments showed similar performance, with a practical LOD in the range of 7–9 ppm.

Even though a small sampling volume of a multicomponent viscous fluid was used without any further sample pre-treatment, GA was detectable with portable devices until 7.66 ppm in case of MiniRAMAN microscope and 8.86 ppm in case of FirstDefender™ RMX. The practical LOD values are lower than the GA LD50 in humans, i.e. 21 $mg\ kg^{-1}$ (ppm). Therefore, this technique would allow, in a near real-life scenario, a fast response and the possibility of employing a portable device for on-site detection of low toxic concentrations.

3.2.2. *Performance assessment in Apolosophy Active + Caffeine Eye Serum*

The SERS performance for the detection of GA in caffeine-based eye serum was then evaluated with three of the four devices. The portable MiniRAMAN microscope was not employed in this case. As for the previous reported case, GA detection was carried out on first design Au NPs, measuring three chips for each concentration and normalizing the recorded intensities by power density and exposure time. Fig. 5a displays GA 2133 cm^{-1} intensity vs. concentration curves in Apolosophy Active + Caffeine Eye Serum with each instrument. As it was the case for the contact lens solution (3.2.1), the SERS signal intensity started to saturate at 50 ppm.

Fig. 5b shows the detection range of the calibration curves collected on the different pieces of equipment, while the detection range of LabRAM 800 H/R is enlarged in Fig. 5c to better illustrate the different intensity scales. A linear correlation between concentration and intensity was obtained between 10 ppm and 50 ppm. In Table S2, linear equation, the R^2, p-value, theoretical LOD, practical LOD, theoretical LOQ, analytical sensitivity, detection range and average RSD values can be found for LabRAM 800 H/R and DXRxi Raman Imaging Microscope. In this second case, FirstDefender™ RMX showed no linear response, since the null hypothesis could not be rejected. The two research-grade equipments showed a theoretical LOD of 0.19 ppm (LabRAM 800 H/R) and 5.85 ppm (DXRxi Raman Imaging Microscope). However, if we analyse the performance considering the practical LOD, the portable device showed once more better performances than the research-grade ones, with a practical LOD of 10.20 ppm. The practical LOD for LabRAM 800 H/R and

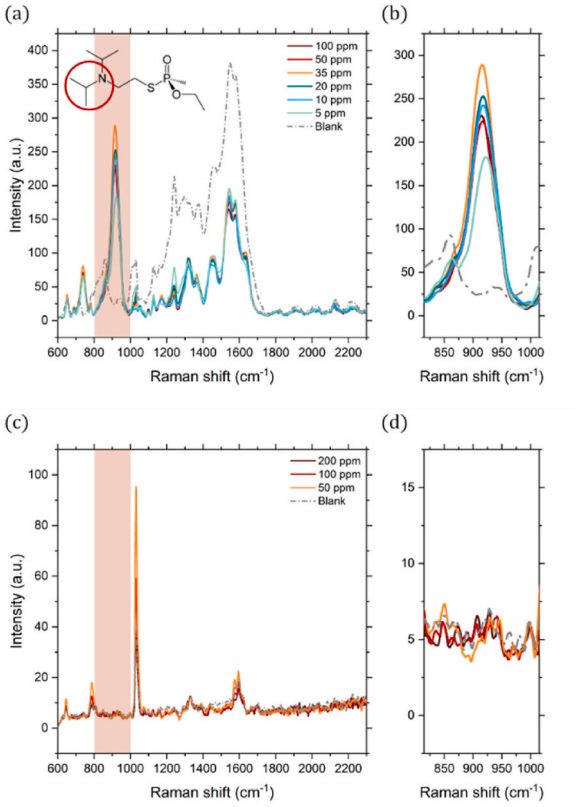

Fig. 6. (a) Averaged SERS spectra after drop casting 3 μl of 100 ppm, 50 ppm, 35 ppm, 20 ppm, 10 ppm, and 5 ppm VX solution in contact lens solution (solid lines) and 3 μl of ACN in contact lens solution (grey dashed line) on Au NP substrates. VX chemical structure is displayed in the inset, highlighting the origin of its characteristic band. (b) Concentration-dependent intensity of the peak at 915 cm^{-1} for VX in contact lens solution. (c) Averaged SERS spectra after drop casting 3 μl of 200 ppm, 100 ppm, and 50 ppm VX solution in eye serum solution (solid lines) and 3 μl of ACN in eye serum solution (grey dashed line) on Au NP substrates. (d) Concentration-dependent intensity of the peak at 915 cm^{-1} for VX in eye serum solution. All spectra were acquired with DXRxi Raman Imaging Microscope (parameters in Table 1).

DXRxi Raman Imaging Microscope are, instead, 18.43 ppm and 21.42 ppm, respectively. The reason for this behaviour could reside in a higher signal intensity of the blank detected from the research-grade instruments. In terms of measurement repeatability, DXRxi Raman Imaging Microscope proved to be the most accurate one, with an RSD between measurements of 11 %, possibly because the intensity is recorded on the entire SERS substrate and the average of 2500 points is considered.

In comparison with GA detection in renu®, higher LOD were obtained for the eye serum matrix, confirming the more intense matrix effect originating from this medium. However, satisfactory LOD were once again obtained, similar to the LD50 in humans (21 $mg\,kg^{-1}$ (ppm)).

3.3. SERS performance evaluation of VX detection in complex matrices

In a second phase, the detection of the V-series nerve agent VX was carried out. As for the previous case, VX was tested in both renu® multi-purpose solution and Apolosophy Active + Caffeine Eye Serum matrices. The averaged SERS spectra of VX can be observed in Fig. 6. The spectra were recorded with DXRxi Raman Imaging Microscope after drop casting 3 μl of 100 ppm, 50 ppm, 35 ppm, 20 ppm, 10 ppm and 5 ppm in contact lens solution (Fig. 6a and b) and 3 μl of 200 ppm, 100 ppm, and 50 ppm in caffeine-based eye serum (Fig. 6c and d). The SERS spectra of VX in the two matrices recorded with the other instruments are shown in supporting information (Figs. S6–S10). The characteristic band of VX at 915 cm^{-1}, which results from CCN stretch or NC_3 stretch vibration [32], is highlighted in Fig. 6a and enlarged in Fig. 6b. Once again, similarly to GA in contact lens solution, VX peak intensity did not linearly increase with concentration, presumably for the same reason as previously explained for GA (3.2).

When VX was diluted in the caffeine-based eye serum, the detection of the compound was not achieved. As evident from Fig. 6c and d, VX peak at 915 cm^{-1} was totally missing from the recorded signal with the research-grade instrument. The reason can be found both in the lower affinity that VX showed for the Au surface, and in the competitive adsorption with caffeine, which displays its characteristic peak at 1032 cm^{-1} very close to VX band and, probably, covering its SERS response. In contrast to GA, VX does not possess any alkyne or cyano group, and consequently it does not display any characteristic peak in the silent region. This makes VX spectrum more susceptible to interfering compounds present in the matrix.

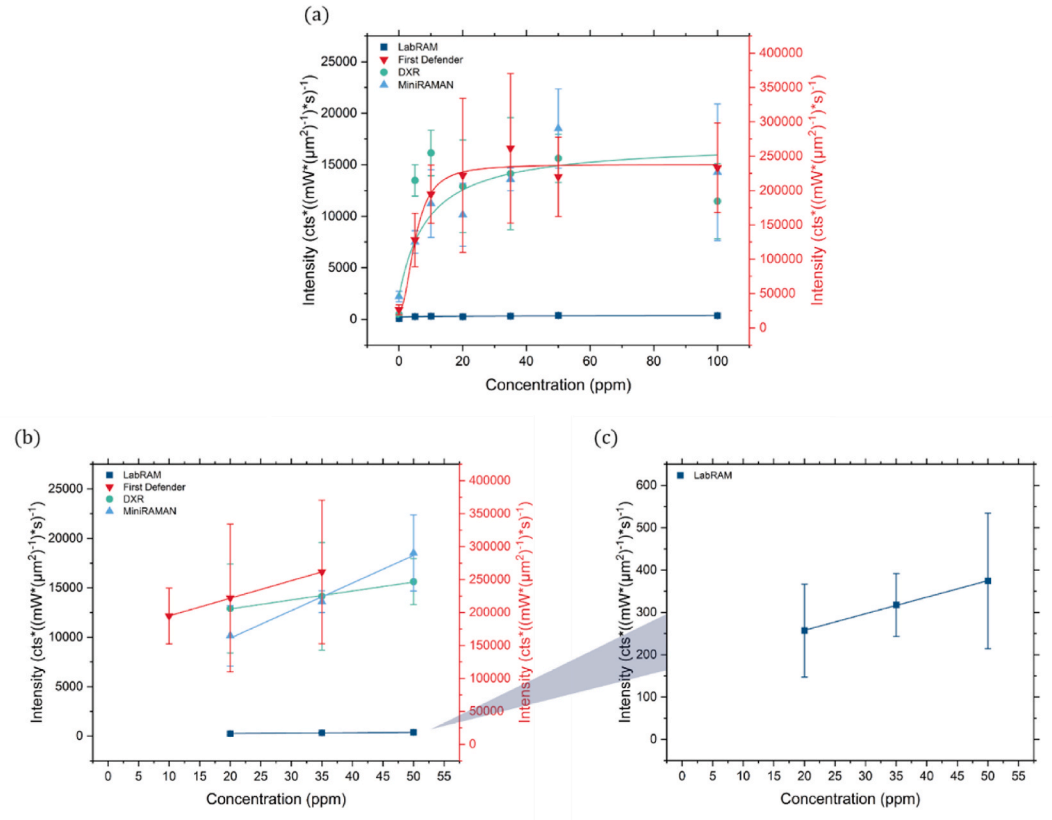

Fig. 7. (a) VX calibration curves in contact lens solution performed using different Raman pieces of equipment. A logistic function was used to fit SERS data. (b) Detection range of the calibration curves. The data acquired with FirstDefender™ RMX are shown in red on the second y-axis. (c) Enlargement of the calibration curve acquired with LabRAM 800 H/R.

3.3.1. Performance assessment in renu® multi-purpose solution

The performance of VX detection in renu® contact lens solution was conducted on AuNPs from the second design. For each concentration, three chips were measured with the four previously mentioned Raman spectrometers and with the parameters listed in Table 1. Fig. 7a shows, for each device, the intensity vs. concentration curve of the 915 cm^{-1} VX band intensity, normalised by power density and exposure time. The SERS signal intensity started to saturate after 35 μM for FirstDefender™ RMX, and after 50 ppm for LabRAM 800 H/R. With the other two pieces of equipment, a significant drop of intensity was already seen at 20 ppm.

Fig. 7b and enlarged Fig. 7c for LabRAM 800 H/R show the detection ranges of the calibration curve for every instrument. Table S3 contains the linear equation, the R^2, p-value, theoretical LOD, practical LOD, theoretical LOQ, analytical sensitivity, detection range and average RSD values for LabRAM 800 H/R, DXRxi Raman Imaging Microscope and FirstDefender™ RMX. As for the previous case of GA in contact lens solution, the MiniRAMAN microscope did not give a linear response, since in the investigation of the p-value the null hypothesis could not be rejected.

LabRAM 800 H/R showed a linear correlation between concentration and intensity from 20 μM to 50 μM with a R^2 of 0.999 and a theoretical LOD and LOQ of 2.07 ppm and 6.89 ppm, respectively. The second research-grade spectrometer, the DXRxi Raman Imaging Microscope, showed the same detection range with an R^2 of 0.997 and a theoretical LOD and LOQ of 5.70 ppm and 19.00 ppm, respectively. With the portable device FirstDefender™ RMX, the detection range spanned from 10 ppm to 35 ppm, with a R^2 of 0.999, a theoretical LOD of 0.75 ppm and a theoretical LOQ of 2.51 ppm. The RSD between measurements varied less in this case, in the range of 22 % (DXRxi Raman Imaging Microscope) to 33 % (FirstDefender™ RMX).

A practical LOD was calculated for all equipments. The practical LODs were in the range of 0.6–7.5 ppm.

When looking at the VX LD50 value for human in liquid form, which is 0.315 $mg\ kg^{-1}$ (ppm), the DXRxi Raman Imaging Microscope was the only instrument that was able to detect VX in that concentration range. The detection of the V-series agent turned out to be much more complicated than the G-agent, probably due to the structure and affinity difference between these two agents.

3.3.2. Performance assessment in Apolosophy Active + Caffeine Eye Serum

The last case is the detection of VX diluted in caffeine-based eye serum. Unfortunately, in this last condition, it was not possible to distinguish the SERS signal of VX from the background. As shown in Fig. 8 and, previously, in the spectral data in Fig. 6c and d, all the three instruments yielded the same results in term of the SERS performance. The high matrix effect, together with an absence of sample pre-treatment probably prevented the analyte reaching close contact with the SERS substrate surface, and therefore did not lead to any signal enhancement.

4. Conclusions

In this study, we evaluated label-free SERS detection performance for two nerve agents in real-life multicomponent fluids. Unfunctionalized commercially available Si-based Au Nanopillar (NP) SERS substrates were employed for the detection of GA and VX in a contact lens solution (renu®), and a caffeine-based eye serum to mimic a possible real-life scenario that involves the dispersion of a nerve agent in everyday life fluids. The SERS performance of two research-grade and two portable Raman spectrometers were compared to assess the possibility of using portable instruments for on-site detection. A strong matrix effect, reducing plasmonic response, was observed, especially for the eye serum. However, GA detection was achieved both in contact lens liquid and in eye serum without any sample pre-treatment. In the first case, a practical LOD in the range of 7–9 ppm was calculated for all pieces of equipment, including the portable devices. These values are lower than the GA LD50 in humans (21 $mg\ kg^{-1}$ or ppm), which demonstrates the potential of using portable Raman spectrometers for on-site detection for a fast response. In eye serum, higher LOD values were obtained for GA with a practical LOD of 10.2 ppm with the portable instrument, and 18.4 ppm and 21.4 ppm with benchtop ones. Due to its lower affinity for Au, VX detection was achieved only in renu® solution, with a practical LOD in the range of 0.6–5 ppm. DXRxi Raman Imaging Microscope was the only instrument able to detect VX in the concentration range of the VX LD50 value for human in liquid form (0.315 $mg\ kg^{-1}$ or ppm). In the last test, VX in eye serum was not detectable probably due to interfering compounds present in the matrix.

In conclusion, a fast and easy detection of nerve agents can be achieved through SERS at significant low toxic concentrations in the range of the percutaneous human LD50. SERS can, thus, represent a promising first line measure for on-site nerve agent testing. For better reproducibility and sensitivity, sample preparation represents a valid option that could be implemented directly on-field. Notably, the use of microfluidic chips for a more systematic and automatized way of handling and wetting the substrates could lead to an improved detection and quantification of nerve agents in liquids with SERS, together with a safer handling of potentially dangerous samples.

Data availability statement

Data will be made available on request.

CRediT authorship contribution statement

Giulia Zappalà: Writing – original draft, Writing – review & editing, Visualization, Validation, Methodology, Investigation, Formal analysis, Data curation, Conceptualization. **Elodie Dumont:** Writing – review & editing, Validation, Supervision, Methodology,

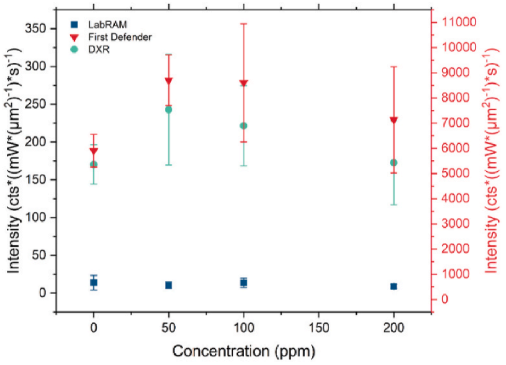

Fig. 8. VX 915 cm^{-1} peak intensity vs. concentration curve in eye serum solution performed using different Raman pieces of equipment. No relation could be observed between intensity and concentration.

Investigation, Formal analysis, Data curation. **Gohar Soufi:** Writing – review & editing, Validation, Methodology, Formal analysis, Data curation. **Nora Molander:** Writing – review & editing, Resources. **Amirali Abbaspourmani:** Writing – review & editing, Methodology. **Damir Asoli:** Writing – review & editing, Methodology, Investigation. **Per Ola Andersson:** Writing – review & editing, Resources. **Tomas Rindzevicius:** Writing – review & editing, Project administration, Funding acquisition. **Anja Boisen:** Writing – review & editing, Resources, Project administration, Funding acquisition.

Declaration of competing interest

The authors declare the following financial interests/personal relationships which may be considered as potential competing interests:Giulia Zappalà reports equipment, drugs, or supplies was provided by Swedish Defence Research Agency. Giulia Zappalà reports equipment, drugs, or supplies was provided by Silmeco ApS. Anja Boisen has patent Surface enhanced Raman scattering substrates consumables for Raman spectroscopy licensed to Technical University of Denmark. If there are other authors, they declare that they have no known competing financial interests or personal relationships that could have appeared to influence the work reported in this paper.

Acknowledgements

The authors acknowledge financial support from the European Union's Horizon 2020 Research and Innovation Programme (Grant Agreement No. 883390 H2020-SU-SECU-2019 SERSing Project), and from BioInnovation Institute Foundation for Therapeutic drug monitoring (Grant Agreement No. NNF20SA0063552) and Roman Slipets (IDUN, Department of Health Technology, Technical University of Denmark, Denmark and BioInnovation Institute Foundation, Copenhagen N, 2200, Denmark) for data analysis software development.

Appendix A. Supplementary data

Supplementary data to this article can be found online at https://doi.org/10.1016/j.heliyon.2024.e32181.

References

[1] K. Kuca, M. Pohanka, Chemical warfare agents, EXS 100 (2010) 543–558.
[2] R.A. Moyer, F.R. Sidell, H. Salem, Nerve agents, Encyclopedia of Toxicology: Third Edition (2014) 483–488, https://doi.org/10.1016/B978-0-12-386454-3.00635-7.
[3] N. Marakovic, et al., Enantioseparation, in vitro testing, and structural characterization of triple-binding reactivators of organophosphate-inhibited cholinesterases, Biochem. J. 477 (2020) 2771–2790.
[4] A. Trang, P.B. Khandhar, Physiology, Acetylcholinesterase. *StatPearls*, 2023.
[5] Y. Lin, J. Wang, G. Liu, C. Timchalk, Portable analytical systems for on-site diagnosis of exposure to pesticides and nerve agents, ACS (Am. Chem. Soc.) Symp. Ser. 1016 (2009) 85–98.
[6] J. Kassa, Review of Oximes in the Antidotal treatment of Poisoning by organophosphorus nerve agents, J. Toxicol. Clin. Toxicol. 40 (2002) 803–816.
[7] N.R. Council, Acute Exposure Guideline Levels for Selected Airborne Chemicals: Volume 3. *Acute Exposure Guideline Levels for Selected Airborne Chemicals*, 2003, https://doi.org/10.17226/10672.
[8] G. Pampalakis, S. Kostoudi, Chemical, Physical, and Toxicological Properties of V-agents, Int. J. Mol. Sci. 24 (2023).
[9] R.A. Moyer, H. Salem, V-series nerve agents: other than VX. Encyclopedia of Toxicology, Third Edition, 2014, pp. 971–975, https://doi.org/10.1016/B978-0-12-386454-3.00668-0.
[10] J.A. Decker, H.W. Rogers, Revised airborne exposure limits for chemical warfare agents. NATO Security through Science Series C: Environmental Security, 2006, pp. 279–287, https://doi.org/10.1007/1-4020-3137-8_31/COVER.

[11] S.D. Cole, K. Willis, H. Salem, F.R. Sidell, Tabun. Encyclopedia of Toxicology, Third Edition, 2014, pp. 462–465, https://doi.org/10.1016/B978-0-12-386454-3.00655-2.
[12] R.A. Moyer, F.R. Sidell, H.V.X. Salem, Encyclopedia of Toxicology (2014) 976–980, https://doi.org/10.1016/B978-0-12-386454-3.00669-2.
[13] K. Ganesan, S.K. Raza, R. Vijayaraghavan, Chemical warfare agents, J. Pharm. BioAllied Sci. 2 (2010) 166.
[14] B. Riley, The toxicology and treatment of injuries from chemical warfare agents, Curr. Anaesth. Crit. Care 14 (2003) 149–154.
[15] A. Vale, T.C. Marrs, P. Rice, Chemical terrorism and nerve agents, Medicine 44 (2016) 106–108.
[16] R.M. Black, R.J. Clarke, R.W. Read, M.T.J. Reid, Application of gas chromatography-mass spectrometry and gas chromatography-tandem mass spectrometry to the analysis of chemical warfare samples, found to contain residues of the nerve agent sarin, sulphur mustard and their degradation products, J. Chromatogr. A 662 (1994) 301–321.
[17] D.B. Mawhinney, et al., The determination of organophosphonate nerve agent metabolites in human urine by hydrophilic interaction liquid chromatography tandem mass spectrometry, J. Chromatogr., B: Anal. Technol. Biomed. Life Sci. 852 (2007) 235–243.
[18] J. Gäb, M. Melzer, K. Kehe, A. Richardt, M.M. Blum, Quantification of hydrolysis of toxic organophosphates and organophosphonates by diisopropyl fluorophosphatase from Loligo vulgaris by in situ Fourier transform infrared spectroscopy, Anal. Biochem. 385 (2009) 187–193.
[19] G.R. Asbury, C. Wu, W.F. Siems, H.H. Hill, Separation and identification of some chemical warfare degradation products using electrospray high resolution ion mobility spectrometry with mass selected detection, Anal. Chim. Acta 404 (2000) 273–283.
[20] F.N. Diauudin, et al., A review of current advances in the detection of organophosphorus chemical warfare agents based biosensor approaches, Sens Biosensing Res 26 (2019) 100305.
[21] C. Chen, W. Zhang, Y. Ke, L. Jiang, X. Hu, A highly sensitive fluorescence probe for on-site detection of nerve agent mimic diethylchlorophosphonate DCP, Anal. Methods 16 (2024) 515–523.
[22] Y. Pan, et al., Environmental characteristics of surface acoustic wave devices for sensing organophosphorus vapor, Sensor. Actuator. B Chem. 315 (2020) 127986.
[23] F. Arduini, A. Amine, D. Moscone, F. Ricci, G. Palleschi, Fast, sensitive and cost-effective detection of nerve agents in the gas phase using a portable instrument and an electrochemical biosensor, Anal. Bioanal. Chem. 388 (2007) 1049–1057.
[24] J. Disley, G. Gil-Ramírez, J. Gonzalez-Rodriguez, A review of sensing technologies for nerve agents, through the use of agent mimics in the gas phase: Future needs, TrAC, Trends Anal. Chem. 168 (2023) 117282.
[25] T.K. Naqvi, et al., Ultra-sensitive reusable SERS sensor for multiple hazardous materials detection on single platform, J. Hazard Mater. 407 (2021) 124353.
[26] Q. Zhao, et al., SERS-based ultrasensitive detection of organophosphorus nerve agents via substrate's surface modification, J. Hazard Mater. 324 (2017) 194–202.
[27] C. Fan, Z. Hu, A. Mustapha, M. Lin, Rapid detection of food- and waterborne bacteria using surface-enhanced Raman spectroscopy coupled with silver nanosubstrates, Appl. Microbiol. Biotechnol. 92 (2011) 1053–1061.
[28] G. Soufi, et al., Discrimination and quantification of methotrexate in the presence of its metabolites in patient serum using SERS mapping, assisted by multivariate spectral data analysis, Biosens. Bioelectron. 14 (2023) 100382.
[29] D.W. Li, W.L. Zhai, Y.T. Li, Y.T. Long, Recent progress in surface enhanced Raman spectroscopy for the detection of environmental pollutants, Microchim. Acta 181 (2014) 23–43.
[30] S.S. Sinha, S. Jones, A. Pramanik, P.C. Ray, Nanoarchitecture based SERS for Biomolecular fingerprinting and label-free Disease Markers diagnosis, Acc. Chem. Res. 49 (2016) 2725–2735.
[31] L. Juhlin, et al., Selective surface-enhanced Raman scattering detection of Tabun, VX and Cyclosarin nerve agents using 4-pyridine amide oxime functionalized gold nanopillars, Talanta 211 (2020) 120721.
[32] S. Farquharson, A. Gift, P. Maksymiuk, F. Inscore, Surface-enhanced Raman spectra of VX and its hydrolysis products, Appl. Spectrosc. 59 (2005) 654–660.
[33] J. Wu, et al., A novel approach for on-site screening of organophosphorus nerve agents based on DTNB modified AgNPs using surface-enhanced Raman spectrometry, Anal. Methods 14 (2022) 4292–4299.
[34] H.K. Lee, et al., Designing surface-enhanced Raman scattering (SERS) platforms beyond hotspot engineering: emerging opportunities in analyte manipulations and hybrid materials, Chem. Soc. Rev. 48 (2019) 731–756.
[35] C.W. Yang, X. Zhang, L. Yuan, Y.K. Wang, G.P. Sheng, Deciphering the microheterogeneous repartition effect of environmental matrix on surface-enhanced Raman spectroscopy (SERS) analysis for pollutants in natural waters, Water Res. 232 (2023) 119668.
[36] renu® multi-purpose contact solution for all day comfort | renu.com. https://www.renu.com/.
[37] Apolosophy Active+ Caffeine Eye Serum 30 ml - Apotek Hjärtat. https://www.apotekhjartat.se/produkt/apolosophy-active-caffeine-eye-serum-30-ml/.
[38] M.S. Schmidt, et al., Large area fabrication of leaning Silicon nanopillars for surface enhanced Raman spectroscopy, Adv. Mater. 24 (2012) OP11–OP18.
[39] K. Wu, et al., Plasmon resonances of Ag capped Si nanopillars fabricated using mask-less lithography, Opt Express 23 (10) (2015) 12965–12978, 12965-12978 **23**.
[40] S.D. Christesen, J.P. Jones, J.M. Lochner, A.M. Hyre, Ultraviolet Raman spectra and cross-Sections of the G-series nerve agents, Appl. Spectrosc. 62 (10) (2008) 1078–1083, 1078-1083 62.
[41] S. Zhang, et al., Raman spectroscopy study of acetonitrile at low temperature, Spectrochim. Acta Mol. Biomol. Spectrosc. 246 (2021) 119065.
[42] R.A. Gu, P.G. Cao, Y.H. Sun, Z.Q. Tian, Surface-enhanced Raman spectroscopy studies of platinum surfaces in acetonitrile solutions, J. Electroanal. Chem. 528 (2002) 121–126.
[43] T. Zhang, et al., Part-per-billion level chemical sensing with a gold-based SERS-active substrate, Sensors 22 (2022).
[44] X. Liu, M. Li, X. Yu, L. Shen, W. Li, Silent region barcode particle arrays for ultrasensitive multiplexed SERS detection, Biosens. Bioelectron. 219 (2023) 114804.